論文 / 著書情報
Article / Book Information

Title	Compression of Fe–Si–H alloys to core pressures
Authors	Shoh Tagawa, Kenji Ohta, Kei Hirose, Chie Kato, Yasuo Oishi
Citation	Geophysical Research Letters, Vol. 43, ,
Pub. date	2016, 3
DOI	http://dx.doi.org/10.1002/2016GL068848
Copyright	(c) 2016 American Geophysical Union (AGU)

AGU PUBLICATIONS

Geophysical Research Letters

RESEARCH LETTER
10.1002/2016GL068848

Key Points:
- Compressibility of hcp $Fe_{0.88}Si_{0.12}H_x$ ($x = 0.61$ and 0.79) was examined up to 138 GPa
- Compression behavior of $Fe_{0.88}Si_{0.12}H_x$ is similar to that of hcp pure Fe and $Fe_{0.88}Si_{0.12}$
- Density profile of $Fe_{0.88}Si_{0.12}H_{0.17}$ matches the PREM for the outer core

Supporting Information:
- Supporting Information S1

Correspondence to:
S. Tagawa,
tagawa.s.aa@m.titech.ac.jp

Citation:
Tagawa, S., K. Ohta, K. Hirose, C. Kato, and Y. Ohishi (2016), Compression of Fe–Si–H alloys to core pressures, *Geophys. Res. Lett.*, *43*, doi:10.1002/2016GL068848.

Received 25 MAR 2016
Accepted 26 MAR 2016
Accepted article online 31 MAR 2016

Compression of Fe–Si–H alloys to core pressures

Shoh Tagawa[1], Kenji Ohta[1], Kei Hirose[2,3], Chie Kato[1], and Yasuo Ohishi[4]

[1]Department of Earth and Planetary Sciences, Tokyo Institute of Technology, Tokyo, Japan, [2]Earth-Life Science Institute, Tokyo Institute of Technology, Tokyo, Japan, [3]Laboratory of Ocean-Earth Life Evolution Research, Japan Agency for Marine-Earth Science and Technology, Kanagawa, Japan, [4]Japan Synchrotron Radiation Research Institute, Hyogo, Japan

Abstract We examined the compression behavior of hexagonal-close-packed (hcp) $(Fe_{0.88}Si_{0.12})_1H_{0.61}$ and $(Fe_{0.88}Si_{0.12})_1H_{0.79}$ (in atomic ratio) alloys up to 138 GPa in a diamond anvil cell (DAC). While contradicting experimental results were previously reported on the compression curve of double-hcp (dhcp) FeH_x ($x \approx 1$), our data show that the compressibility of hcp $Fe_{0.88}Si_{0.12}H_x$ alloys is very similar to those of hcp Fe and $Fe_{0.88}Si_{0.12}$, indicating that the incorporation of hydrogen into iron does not change its compression behavior remarkably. The present experiments suggest that the inner core may contain up to 0.47 wt % hydrogen ($FeH_{0.26}$) if temperature is 5000 K. The calculated density profile of $Fe_{0.88}Si_{0.12}H_{0.17}$ alloy containing 0.32 wt % hydrogen in addition to geochemically required 6.5 wt % silicon matches the seismological observations of the outer core, supporting that hydrogen is an important core light element.

1. Introduction

Birch [1952] first reported that the density of the Earth's outer core is substantially lower than that of pure iron, but the identification of light elements that are responsible for such a density deficit is still an open question. Several light elements such as H, C, O, Si, and S have been proposed on the basis of high-pressure mineral physics data and cosmochemical/geochemical arguments. Fe–H alloy has been studied the least among possible core alloys [see *Hirose et al*., 2013, Figure 1] but has recently gained more attention, in part because planet formation theory suggests that a large amount of water may have been brought to the Earth during its formation due to gravitational scattering of H_2O-bearing planetesimals by Jupiter [*Morbidelli et al*., 2000]. Indeed, such an effect has been enhanced if Jupiter migrated inward in the early stage of Earth's formation [*Walsh et al*., 2011]. *Hui et al*. [2013] found a certain amount of water in lunar plagioclase, suggesting that the lunar (and thus terrestrial) magma ocean already contained H_2O that survived giant impact events [*Genda and Abe*, 2005; *Hamano et al*., 2013]. It is also known that hydrogen is a strong siderophile element. *Okuchi* [1997] argued that most of the H_2O in the magma ocean may have been incorporated into metals as hydrogen. More recently, *Nomura et al*. [2014] suggested the presence of hydrogen in the core in order for the outer core to be molten under relatively low temperature. Note that the solidus temperature of FeH is ~2600 K at the core-mantle boundary (CMB) [*Sakamaki et al*., 2009], which is even lower than the ~3000 K for the eutectic temperature in the Fe–FeS binary system [*Morard et al*., 2008].

So far, the effect of hydrogen on the property of iron and iron alloy is little known. FeH_x ($x \approx 1$) is easily formed under hydrogen-saturated conditions and has been examined repeatedly by high-pressure experiments [e.g., *Badding et al*., 1991; *Hirao et al*., 2004; *Pépin et al*., 2014]. By contrast, there are only a few experimental studies on FeH_x ($x < 1$) [*Yamakata et al*., 1992; *Antonov et al*., 1998], regardless of the fact that the core density deficit is explained by FeH_x with $x = 0.28$–0.56 [*Narygina et al*., 2011] or $x = 0.55$–1.12 [*Terasaki et al*., 2012].

Stable crystal structures of FeH_x are also not understood yet; the double-hexagonal-close-packed (dhcp) phase is formed at room temperature above 3.5 GPa [*Badding et al*., 1991] and preserved up to at least 136 GPa [*Pépin et al*., 2014]. On the other hand, the ab initio calculations by *Isaev et al*. [2007] suggested that the face-centered-cubic (fcc) phase of FeH_x ($x = 1$) is stable above 83 GPa. Such fcc FeH_x was indeed synthesized at 54 GPa and 1650 K by *Narygina et al*. [2011]. *Yamakata et al*. [1992] reported the formation of hcp FeH_x ($x < 1$) from body-centered-cubic (bcc) Fe around 400°C and 6 GPa, and *Antonov et al*. [1998] performed neutron diffraction measurements on nonmagnetic hcp $FeD_{0.42\pm0.04}$ at 1 bar and 90 K. Previous reports on the compression behavior of FeH_x were inconsistent with each other; *Hirao et al*. [2004] showed that dhcp FeH_x ($x \approx 1$) became much stiffer than pure iron after magnetic transition above 50 GPa, whereas the similar room temperature compression experiments by *Pépin et al*. [2014] found its compressibility to be more than that of pure iron.

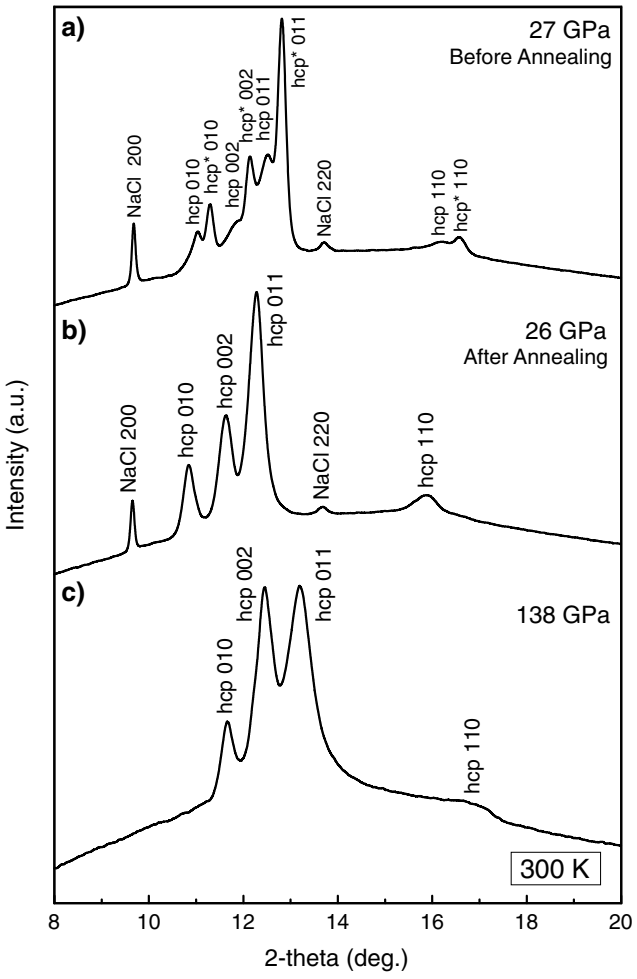

Figure 1. Integrated XRD patterns collected at room temperature during run #1; (a) before and (b) after thermally annealing around 26 GPa and (c) at 138 GPa, the highest pressure condition in this study. Two hcp phases were found in Figure 1a before thermal annealing, and they became single upon heating (Figure 1b).

In addition to hydrogen, silicon has been considered to be an important light element in the core from cosmochemical and geochemical studies. The high Mg/Si ratio of the Earth's mantle compared to that of solar abundance suggested ~7 wt % Si in the core [*Allègre et al.*, 1995]. Moreover, the difference in Si isotopic composition between mantle and chondrites also supports ~6 wt % Si in the core [e.g., *Georg et al.*, 2007; *Shahar et al.*, 2009].

In this study, we examined hydrogen-bearing Fe–6.5wt %Si alloy ($Fe_{0.88}Si_{0.12}H_{0.61}$ and $Fe_{0.88}Si_{0.12}H_{0.79}$ in atomic ratio) at high pressures in a diamond anvil cell (DAC). Previous study on Fe–Si–H alloy was limited to the FeSi–H system at low pressures [*Terasaki et al.*, 2011]. In this paper, the hydrogenation, crystal structure, volume, and compression behavior of Fe–Si–H alloys are reported up to 138 GPa. We also discuss the presence of hydrogen and its abundance in the core based on these new data.

2. Experimental Method

In order to examine the crystal structure and compression behavior of iron-rich Fe–Si–H alloys, we performed in situ X-ray diffraction measurements up to 138 GPa using laser-heated diamond anvil cell technique. Two sets of experiments were carried out using diamond anvils with a culet size of 120 μm (run #1) or 150 μm (run # 2). We used Re gaskets preindented to about 20 μm thick. So as to prevent hydrogen embrittlement of the Re gasket and the escape of hydrogen from a sample chamber, a NaCl inner gasket was prepared with a Focused Ion Beam (FIB, Versa 3-D, *FEI*). The surface of the diamond anvils was coated with a thin layer of Ti by sputtering [*Ohta et al.*, 2015]. Approximately 5 μm thick $Fe_{0.88}Si_{0.12}$ (6.5 wt % Si) foil (99.99% purity, *Rare Metallic*) was put into the sample chamber, together with a small NaCl plate that was used as a pressure marker. A ruby ball was additionally used in run #2. We then loaded hydrogen using a liquid hydrogen-introducing system at temperatures below 20 K [*Chi et al.*, 2011]. The sample and hydrogen were compressed under low temperature and subsequently restored to room temperature. A pressure-temperature path before thermal annealing was monitored with pressure measurement using ruby (3000 ppm Cr^{3+}, *P.M.C.*) in the second run; we compressed the sample to 13 GPa at 150 K from 1.0 GPa below 80 K, and then temperature was returned to 280 K. The presence of hydrogen in the sample chamber was confirmed by Raman spectroscopy; we observed a signal from the vibron of H_2 molecules in both runs. After compression to 27 GPa (run #1) and 62 GPa (run #2) at room temperature, Fe–Si foils were heated from both sides with Yb fiber lasers for 17 and 74 min in runs #1 and #2, respectively, in order to promote their hydrogenation. Annealing temperature was ~1000 K.

X-ray diffraction (XRD) patterns were obtained at BL10XU, SPring-8 [*Ohishi et al.*, 2008]. The incident X-ray beam was monochromatized to a wavelength of 0.4143–0.4159 Å (~30 keV) and focused to 6 μm in diameter.

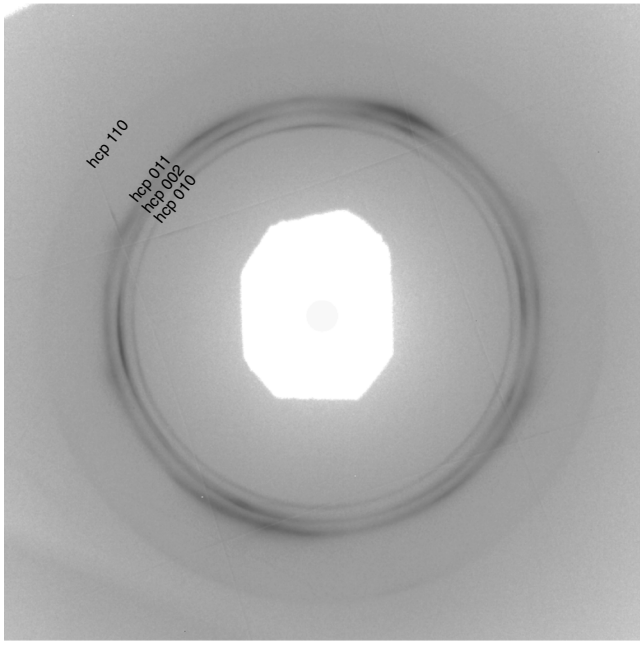

Figure 2. Two-dimensional XRD pattern of $Fe_{0.88}Si_{0.12}H_{0.61}$ at 138 GPa (see text for details).

To collect diffraction data, we used a flat panel X-ray detector (*PerkinElmer*) with exposure time of 1 s. Pressure was determined from the volume of NaCl on the basis of its equation of state (EoS) for the B1 [*Matsui et al.*, 2012] and B2 structures [*Sata et al.*, 2002]. The EoS of B2 NaCl is based on the MgO pressure scale that was also used for previous experiments on hcp Fe-Si alloy [*Tateno et al.*, 2015]. In run #1, we collected XRD measurements separately for a sample and for a pressure marker in order to avoid peak overlapping above 52 GPa. We found that the pressure gradient in a sample chamber was small, at most 2 GPa through the present experiments.

3. Results

3.1. Hydrogenation and Crystal Structure of Fe–Si–H

The hcp phase appeared at high pressure in both runs before thermal annealing (Figure 1). The crystal structure did not change upon thermal annealing although volumes increased due to hydrogenation. The hcp phase was preserved up to 138 GPa. It contrasts the Fe–H system, in which the dhcp phase was formed from bcc upon compression to >3.5 GPa at 300 K [*Badding et al.*, 1991; *Hirao et al.*, 2004]. The dhcp phase is distinguished from hcp by additional dhcp 011, 013, and 015 peaks, but these peaks were not found in our experiments (Figure 1). In run #1, a couple of hcp phases were observed at 27 GPa before heating. One exhibited a volume very similar to that of $Fe_{0.88}Si_{0.12}$ (Fe–6.5wt %Si) at equivalent pressure calculated from those of pure Fe [*Dewaele et al.*, 2006] and hcp Fe–9wt%Si [*Tateno et al.*, 2015] (note that pressures in this study and Tateno et al. are both based on the MgO pressure scale), and the other had a larger volume because of the incorporation of hydrogen. After thermally annealing, only the single hcp phase was found with a volume larger than those before heating, which indicated further hydrogenation (Figure 1). The XRD data were first collected at 20 GPa in run #2, where only the single hcp phase was observed before heating. As described in section 3.3, the hydrogen concentrations were $Fe_{0.88}Si_{0.12}H_{0.61}$ and $Fe_{0.88}Si_{0.12}H_{0.79}$ (in atomic ratio) in runs #1 and #2, respectively.

The XRD pattern obtained in this study showed two characteristics. First, the hcp 002 peak was strong for Fe–Si–H (Figure 1), while it is known to be weak for pure Fe and iron-rich Fe–Si alloy in which the (001) plane aligned perpendicular to a compression direction. Second, Fe–Si–H developed strong preferred orientation (Figure 2). These suggest that hydrogenation changes the dominant slip system and deformation mechanism of the hcp phase.

3.2. Compression Behavior

Pressure-volume data were collected for hcp $Fe_{0.88}Si_{0.12}H_{0.61}$ in a pressure range from 26 to 138 GPa (run #1) and for $Fe_{0.88}Si_{0.12}H_{0.79}$ from 63 to 127 GPa (run #2) (Figure 3 and Table S1 in the supporting information). We examined the compression behaviors of these Fe–Si–H alloys by fitting the Vinet EoS to the data:

$$P = 3K_0\left(\frac{V}{V_0}\right)^{-\frac{2}{3}}\left[1-\left(\frac{V}{V_0}\right)^{\frac{1}{3}}\right]\exp\left\{\frac{2}{3}\left(K_0'-1\right)\left[1-\left(\frac{V}{V_0}\right)^{\frac{1}{3}}\right]\right\} \quad (1)$$

For $Fe_{0.88}Si_{0.12}H_{0.61}$ in run #1, we obtained bulk modulus at ambient condition $K_0 = 223 \pm 11$ GPa, its pressure derivative $K_0' = 4.8 \pm 0.2$, and volume at 1 bar $V_0 = 24.96 \pm 0.08$ Å^3 per hcp unit cell (Table 1). Since the pressure range of volume measurement was limited in the second run, we fixed its V_0 (see section 3.3) and $K_0' = 4.8$ and found $K_0 = 234 \pm 1$ GPa for $Fe_{0.88}Si_{0.12}H_{0.79}$.

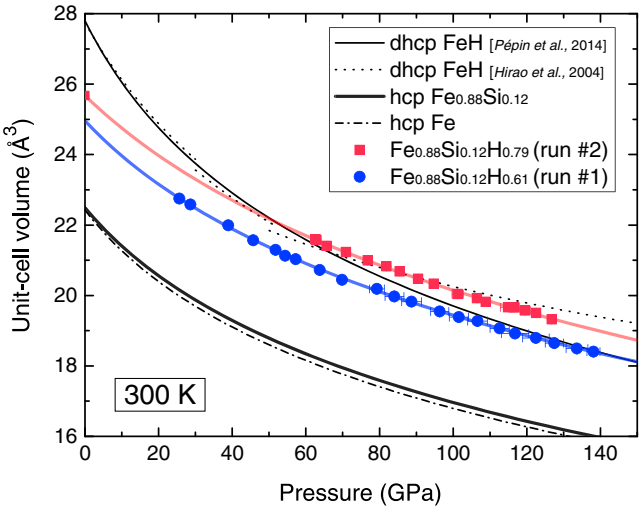

Figure 3. Compression curves of hcp $Fe_{0.88}Si_{0.12}H_{0.61}$ (blue, run #1) and $Fe_{0.88}Si_{0.12}H_{0.79}$ (red, run #2). Previous data on dhcp FeH by *Hirao et al.* [2004] (dotted curve) and by *Pépin et al.* [2014] (thin solid curve) are given for comparison. The compression curves of hcp Fe (dash dot curve) [*Dewaele et al.*, 2006] and $Fe_{0.88}Si_{0.12}$ (thick solid curve) [*Tateno et al.*, 2015] are also shown as references. The half of the unit cell volume is given for dhcp FeH.

The compression behavior of these $Fe_{0.88}Si_{0.12}H_x$ alloys is found to be different from that of FeH_x ($x \approx 1$) examined in two previous experimental studies (Figure 3). *Hirao et al.* [2004] reported that FeH_x became much stiffer than iron after transition to a nonmagnetic state (>50 GPa), while the more recent work by *Pépin et al.* [2014] showed FeH_x is more compressible than iron up to 136 GPa. Our data on $Fe_{0.88}Si_{0.12}H_x$ demonstrate that its compression behavior is very similar to that of pure iron [*Dewaele et al.*, 2006] and $Fe_{0.88}Si_{0.12}$ [*Tateno et al.*, 2015] (Figure 3), although Fe–Si–H alloys have larger K_0 but smaller K_0' (Table 1). The volume difference between $Fe_{0.88}Si_{0.12}$ and $Fe_{0.88}Si_{0.12}H_{0.61}$ is 12.7% at 100 GPa and 13.5% at 300 GPa.

3.3. Hydrogen Concentration in hcp Fe–Si–H

We estimated the hydrogen content of $Fe_{0.88}Si_{0.12}H_{0.61}$ synthesized in the first run on the basis of its V_0 value obtained by EoS fitting and the volume of hydrogen V_H at ambient pressure. *Antonov et al.* [1998] reported the volume of nonmagnetic hcp $FeD_{0.42}$ from neutron diffraction measurements. The volume difference between hcp iron [*Dewaele et al.*, 2006] and hcp $FeD_{0.42}$ gives $V_H = 2.017$ Å^3 at 1 bar. Note that the volume of deuterium is very similar to that of hydrogen [*Antonov et al.*, 1998]. This value is consistent with the volume of deuterium (2.21 ± 0.04 Å^3) in fcc $FeD_{0.64}$ at 6.3 GPa at 988 K recently measured by *Machida et al.* [2014]. It is also similar to the V_H observed in other 3*d* transition metals such as Cr, Mn, Co, Ni, and Mo [*Sakamaki et al.*, 2009; *Machida et al.*, 2014]. On the other hand, this value is much smaller than $V_H = 2.96$ Å^3 [*Fukai*, 1992], which has often been used to estimate hydrogen concentrations in FeH_x

Table 1. EoS Parameters for $Fe_{0.88}Si_{0.12}H_x$ and Related Metals

	Unit Cell V_0 (Å3)	K_0 (GPa)	K_0'	EoS[a]	
		hcp Fe–Si–H			
$Fe_{0.88}Si_{0.12}H_{0.61}$	24.96(8)	223(11)	4.8(2)	V	This study
$Fe_{0.88}Si_{0.12}H_{0.79}$	25.67(fix)	234(1)	4.8(fix)	V	This study
	25.67(fix)	253(4)	4.2(2)	V	This study
		dhcp FeH_x			
$FeH_{x \approx 1}$	50.76[b]	182(45)	8.5(2.9)	BM	*Hirao et al.* [2004] (≥50 GPa)
	55.60(20)[b]	131.1(3.0)	4.83	V	*Pépin et al.* [2014]
		hcp FeH_x			
$FeH_{0.5}$	23.57	244.2	4.277	BM	*Caracas* [2015]
$FeH_{1.0}$	25.97	224.8	4.203	BM	*Caracas* [2015]
		hcp Fe–Si			
$Fe_{0.88}Si_{0.12}$	22.49	177.8(1.5)	5.07(5)	V	*Tateno et al.* [2015][c]
		hcp Fe			
Fe	22.43(10)	163.4(7.9)	5.38(16)	V	*Dewaele et al.* [2006]

[a]V, Vinet; BM, third order Birch-Murnaghan.
[b]$Z = 4$.
[c]EoS parameters are obtained from the volumes calculated by linear interpolation between those of pure hcp Fe [*Dewaele et al.*, 2006] and hcp Fe–9wt%Si [*Tateno et al.*, 2015]. Pressure was recalculated using MgO pressure scale by *Speziale et al.* [2001].

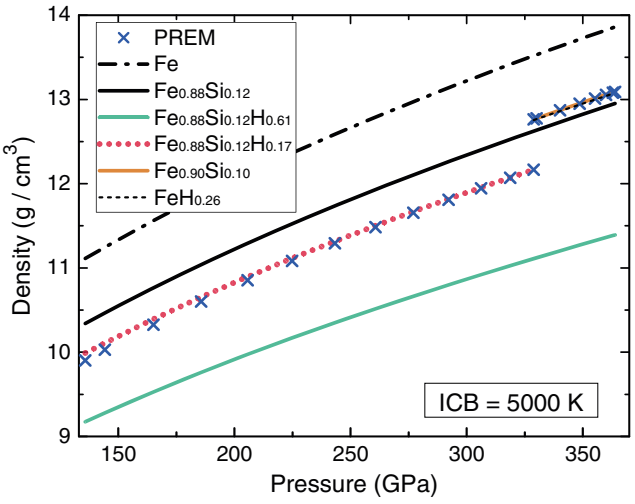

Figure 4. Comparison of the density of $Fe_{0.88}Si_{0.12}H_{0.17}$ alloy (red dotted curve) along isentropic temperature profile ($T_{ICB} = 5000$ K) with the PREM density (cross mark). The density profiles of Fe [*Dewaele et al.*, 2006] (dash dot curve), $Fe_{0.88}Si_{0.12}$ [*Tateno et al.*, 2015] (black solid curve), and $Fe_{0.88}Si_{0.12}H_{0.61}$ (this study, run #1, green solid curve) are also shown. The densities of $Fe_{0.90}Si_{0.10}$ and $FeH_{0.26}$ match the PREM value for the inner core.

[*Terasaki et al.*, 2011, 2012] (see supporting information). The hydrogen content x in $Fe_{0.88}Si_{0.12}H_x$ is defined using $x = [V(Fe_{0.88}Si_{0.12}H_x) - V(Fe_{0.88}Si_{0.12})]/2V_H$ (note the number of formula unit in hcp lattice $Z = 2$). Using $V_H = 2.017$ Å^3 and $V_0 = 22.49$ Å^3 for hcp $Fe_{0.88}Si_{0.12}$ [*Tateno et al.*, 2015], the composition of the alloy synthesized in run #1 is calculated to be $Fe_{0.88}Si_{0.12}H_{0.61}$ (atomic ratio) from its $V_0 = 24.96$ Å^3.

For the second run, the hydrogen concentration was estimated from $V_H(P)$ because V_0 is not well constrained by the EoS fitting. First, we obtained $V_H(P)$ as a function of pressure from the difference in volume between $Fe_{0.88}Si_{0.12}H_{0.61}$ (run #1) and $Fe_{0.88}Si_{0.12}$ [*Tateno et al.*, 2015], assuming that the hydrogen concentration was constant throughout the first run. With such $V_H(P)$, the hydrogen content in run #2 was calculated to be $x = 0.79 \pm 0.02$ between 63 and 127 GPa. Indeed, such constant x value supports that the hydrogen contents did not change during compression after thermal annealing in both runs. The $x = 0.79$ indicates $V_0 = 25.67$ Å^3 for $Fe_{0.88}Si_{0.12}H_{0.79}$ in run #2. Using this V_0 value, we obtain its EoS parameters (see above).

It is noted that x was less than 1.0 in both runs #1 and #2 even after thermal annealing under hydrogen-saturated conditions. It suggests that the octahedral sites of the hcp lattice were not fully occupied by hydrogen, in contrast to the case of dhcp FeH_x ($x \approx 1$) [*Hirao et al.*, 2004; *Pépin et al.*, 2014].

4. Fe–Si–H Alloy in the Core?

The densities of silicon/hydrogen-bearing iron alloys are estimated for both inner and outer core conditions using the EoS parameters obtained for $Fe_{0.88}Si_{0.12}H_{0.61}$ and $Fe_{0.88}Si_{0.12}$ listed in Table 1. Here we consider isentropic temperature profile for the outer core, which is given by

$$T = T_{ICB}\left(\frac{\rho}{\rho_{ICB}}\right)^{\gamma} \quad (2)$$

where ρ is density and $\gamma = 1.5$ is Grüneisen parameter [*Vočadlo et al.*, 2003]. The thermal expansivity of Fe–Si–H is assumed to be the same as that for iron reported by *Dewaele et al.* [2006]. We first calculated the hydrogen concentrations that match the densities observed for the inner and outer core sides of the inner core boundary (ICB) [*Dziewonski and Anderson*, 1981] when temperature is 5000 K [*Hirose et al.*, 2013]. The results show that the maximum amount of hydrogen in the inner core is 0.47 wt % ($FeH_{0.26}$ in atomic ratio). On the other hand, if silicon is a single light element, the inner core density is explained by $Fe_{0.90}Si_{0.10}$ (5.4 wt % Si). Considering geochemically proposed 6.5 wt % Si for the outer core [e.g., *Georg et al.*, 2007; *Shahar et al.*, 2009], we obtain $Fe_{0.88}Si_{0.12}H_{0.17}$ (0.32 wt % H). In these calculations, we assumed ideal volume mixing between $Fe_{0.88}Si_{0.12}$ and $Fe_{0.88}Si_{0.12}H_x$. While solid data are used for these calculations for the outer core, previous shock wave compression experiments [*Brown and McQueen*, 1986] and ab initio calculations [*Ichikawa et al.*, 2014] reported that the volume difference between solid and liquid iron is about 2% at the outer core pressure range. Nevertheless, such difference is indeed comparable to the resolution of density determinations from seismological observations. *Masters and Gubbins* [2003] argued that the resolution is no better than 1% when averaged over a depth width of 270 km in the lowermost outer core, suggesting that the uncertainty in the outer core preliminary reference Earth model (PREM) density is larger than 1.6% near the ICB.

The densities of $Fe_{0.90}Si_{0.10}/FeH_{0.26}$ and $Fe_{0.88}Si_{0.12}H_{0.17}$ were then calculated over the entire inner and outer core pressure range, respectively, along the isentropic temperature curve with the ICB temperature of 5000 K. The compressibility of these alloys is in good agreement with the PREM density profile for both inner and outer cores (Figure 4). The deviation is only 0.86% at the CMB, which is smaller than the observational uncertainty of 2.4% at the topmost core [*Masters and Gubbins*, 2003]. Additionally, we calculated the hydrogen contents and the density profiles of Fe–Si–H alloys, considering higher ICB temperatures of 5500 and 6000 K (Figures S1 and S2 in the supporting information). The consistency between these calculated density profiles and the PREM values becomes even better with increasing temperature.

If the outer core composition is $Fe_{0.88}Si_{0.12}H_{0.17}$, the total amount of hydrogen in the core is 38 times as much as that of seawater, suggesting that a large volume of water was brought to the Earth during planet formation and incorporated into metals in a magma ocean [*Okuchi*, 1997]. If only hydrogen was dissolved into the core, oxygen formed iron oxide from metal. Alternatively, it is also possible that oxygen was incorporated into metals jointly with hydrogen and later exsolved as SiO_2 from the core [*Hirose et al*., 2015]. Indeed, previous simulations showed that 17–66 times [*Raymond et al*., 2007] or 13–46 times seawater [*Walsh et al*., 2011] was supplied to the Earth, which is in agreement with the $Fe_{0.88}Si_{0.12}H_{0.17}$ core composition. The melting temperature of such a Fe–Si–H core should be substantially lower than that of pure Fe [*Sakamaki et al*., 2009], consistent with the relatively low core temperature (3600 K at the CMB) inferred from recent measurements of the solidus temperature of the lowermost mantle [*Nomura et al*., 2014].

5. Conclusions

We studied the compression behavior of $Fe_{0.88}Si_{0.12}H_x$ alloys (6.5 wt % Si) with two different hydrogen concentrations, $x = 0.61$ and 0.79 in atomic ratio (1.2 and 1.5 wt % H), to 138 GPa at room temperature in a DAC. Hydrogenation of Fe–Si alloys mainly occurred upon thermal annealing to ~1000 K at 27–62 GPa in this study. While dhcp FeH_x ($x \approx 1$) was reported in previous experiments, we observed the hcp phase for $Fe_{0.88}Si_{0.12}H_x$ alloys. It was once argued that FeH_x ($x \approx 1$) became stiffer than pure iron after transition to a nonmagnetic state above 50 GPa, but more recent experiments showed that FeH_x alloy is more compressible than iron. In contrast, our data demonstrate that the compressibility of $Fe_{0.88}Si_{0.12}H_x$ alloys is very similar to that of iron and $Fe_{0.88}Si_{0.12}$, indicating that the incorporation of hydrogen into iron does not change its compression behavior.

We further estimated the hydrogen concentrations in the Earth's core. The inner core may include up to 0.47 wt % H ($FeH_{0.26}$ in atomic ratio) when the ICB temperature is 5000 K. The PREM density profile of the outer core is explained with iron containing 0.32 wt % hydrogen in addition to geochemically proposed 6.5 wt % silicon ($Fe_{0.88}Si_{0.12}H_{0.17}$), supporting the Fe–Si–H core composition. It suggests that an extensive amount of water, 38 times as much as seawater, may have been brought to the Earth during its formation, consistent with recent planet formation simulations considering the inward migration of Jupiter.

Acknowledgments
Data supporting Figure 3 are available as supporting information Table S1. Discussion with G. Helffrich on the uncertainty in core density observations was very useful. We thank S. Tateno for his support in our experiment. Comments from reviewers were helpful to improve the manuscript. Synchrotron XRD measurements were made at BL10XU, SPring-8 (proposals 2014A0080, 2014B0080, and 2015A0080).

References

Allègre, C. J., J.-P. Poirier, E. Humler, and A. W. Hofmann (1995), The chemical composition of the Earth, *Earth Planet. Sci. Lett.*, *134*, 515–526, doi:10.1016/0012-821X(95)00123-T.

Antonov, V. E., K. Cornell, V. K. Fedotov, A. I. Kolesnikov, E. G. Ponyatovsky, V. I. Shiryaev, and H. Wipf (1998), Neutron diffraction investigation of the dhcp and hcp iron hydrides and deuterides, *J. Alloys Compd.*, *264*, 214–222, doi:10.1016/S0925-8388(97)00298-3.

Badding, J. V., R. J. Hemley, and H.-K. Mao (1991), High-pressure chemistry of hydrogen in metals: In situ study of iron hydride, *Science*, *253*, 421–424, doi:10.1126/science.253.5018.421.

Birch, F. (1952), Elasticity and constitution of the Earth's interior, *J. Geophys. Res.*, *57*, 227–286, doi:10.1029/JZ057i002p00227.

Brown, J. M., and R. G. McQueen (1986), Phase transitions, Grüneisen parameter, and elasticity for shocked iron between 77 GPa and 400 GPa, *J. Geophys. Res.*, *91*, 7485–7494, doi:10.1029/JB091iB07p07485.

Caracas, R. (2015), The influence of hydrogen on the seismic properties of solid iron, *Geophys. Res. Lett.*, *42*, 3780–3785, doi:10.1002/2015GL063478.

Chi, Z., H. Nguyen, T. Matsuoka, T. Kagayama, N. Hirao, Y. Ohishi, and K. Shimizu (2011), Cryogenic implementation of charging diamond anvil cells with H_2 and D_2, *Rev. Sci. Instrum.*, *82*, 105109, doi:10.1063/1.3652981.

Dewaele, A., P. Loubeyre, F. Occelli, M. Mezouar, P. I. Dorogokupets, and M. Torrent (2006), Quasihydrostatic equation of state of iron above 2 Mbar, *Phys. Rev. Lett.*, *97*, 215504, doi:10.1103/PhysRevLett.97.215504.

Dziewonski, A. M., and D. L. Anderson (1981), Preliminary reference Earth model, *Phys. Earth Planet. Inter.*, *25*, 297–356, doi:10.1016/0031-9201(81)90046-7.

Fukai, Y. (1992), Some properties of the Fe-H system at high pressures and temperatures, and their implications for the Earth's core, in *High-Pressure Res: Appl. to Earth Planet. Sci*., vol. 67, 373–385, TERRAPUB, Washington D. C., doi:10.1029/GM067p0373.

Genda, H., and Y. Abe (2005), Enhanced atmospheric loss on protoplanets at the giant impact phase in the presence of oceans, *Nature*, *433*, 842–844, doi:10.1038/nature03360.

Georg, R. B., A. N. Halliday, E. A. Schauble, and B. C. Reynolds (2007), Silicon in the Earth's core, *Nature*, *447*, 1102–1106, doi:10.1038/nature05927.

Hamano, K., Y. Abe, and H. Genda (2013), Emergence of two types of terrestrial planet on solidification of magma ocean, *Nature*, *497*, 607–610, doi:10.1038/nature12163.

Hirao, N., T. Kondo, E. Ohtani, K. Takemura, and T. Kikegawa (2004), Compression of iron hydride to 80 GPa and hydrogen in the Earth's inner core, *Geophys. Res. Lett.*, *31*, L06616, doi:10.1029/2003GL019380.

Hirose, K., S. Labrosse, and J. Hernlund (2013), Composition and state of the core, *Annu. Rev. Earth Planet. Sci.*, *41*, 657–691, doi:10.1146/annurev-earth-050212-124007.

Hirose, K., G. Morard, J. W. Hernlund, G. R. Helffrich, and H. Ozawa (2015), Crystallization in Earth's core after high-temperature core formation, Abstract presented at AGU Fall Meeting 2015, AGU, San Francisco, Calif.

Hui, H., A. H. Peslier, Y. Zhang, and C. R. Neal (2013), Water in lunar anorthosites and evidence for a wet early Moon, *Nat. Geosci.*, *6*, 177–180, doi:10.1038/ngeo1735.

Ichikawa, H., T. Tschuchiya, and Y. Tange (2014), The P-V-T equation of state and thermodynamic properties of liquid iron, *J. Geophys. Res. Solid Earth*, *119*, 240–252, doi:10.1002/2013JB010732.

Isaev, E. I., N. V. Skorodumova, R. Ahuja, Y. K. Vekilov, and B. Johansson (2007), Dynamical stability of Fe-H in the Earth's mantle and core regions, *Proc. Natl. Acad. Sci. U.S.A.*, *104*, 9168–9171, doi:10.1073/pnas.0609701104.

Machida, A., et al. (2014), Site occupancy of interstitial deuterium atoms in face-centred cubic iron, *Nat. Commun.*, *5*, 5063, doi:10.1038/ncomms6063.

Masters, G., and D. Gubbins (2003), On the resolution of density within the Earth, *Phys. Earth Planet. Inter.*, *140*, 159–167, doi:10.1016/j.pepi.2003.07.008.

Matsui, M., Y. Higo, Y. Okamoto, T. Irifune, and K.-I. Funakoshi (2012), Simultaneous sound velocity and density measurements of NaCl at high temperatures and pressures: Application as a primary pressure standard, *Am. Mineral.*, *97*, 1670–1675, doi:10.2138/am.2012.4136.

Morard, G., D. Andrault, N. Guignot, C. Sanloup, M. Mezouar, S. Petitgirard, and G. Fiquet (2008), In situ determination of Fe–Fe_3S phase diagram and liquid structural properties up to 65 GPa, *Earth Planet. Sci. Lett.*, *272*, 620–626, doi:10.1016/j.epsl.2008.05.028.

Morbidelli, A., J. Chambers, J. I. Lunine, J. M. Petit, F. Robert, G. B. Valsecchi, and K. E. Cyr (2000), Source regions and timescales for the delivery of water to the Earth, *Meteorit. Planet. Sci.*, *35*, 1309–1320, doi:10.1111/j.1945-5100.2000.tb01518.x.

Narygina, O., L. S. Dubrovinsky, C. A. McCammon, A. Kurnosov, I. Y. Kantor, V. B. Prakapenka, and N. A. Dubrovinskaia (2011), X-ray diffraction and Mössbauer spectroscopy study of fcc iron hydride FeH at high pressures and implications for the composition of the Earth's core, *Earth Planet. Sci. Lett.*, *307*, 409–414, doi:10.1016/j.epsl.2011.05.015.

Nomura, R., K. Hirose, K. Uesugi, Y. Ohishi, A. Tsuchiyama, A. Miyake, and Y. Ueno (2014), Low core–mantle boundary temperature inferred from the solidus of pyrolite, *Science*, *343*, 522–525, doi:10.1126/science.1248186.

Ohishi, Y., N. Hirao, N. Sata, K. Hirose, and M. Takata (2008), Highly intense monochromatic X-ray diffraction facility for high-pressure research at SPring-8, *High Press. Res.*, *28*, 163–173, doi:10.1080/08957950802208910.

Ohta, K., K. Ichimaru, M. Einaga, S. Kawaguchi, K. Shimizu, T. Matsuoka, N. Hirao, and Y. Ohishi (2015), Phase boundary of hot dense fluid hydrogen, *Sci. Rep.*, *5*, 16560, doi:10.1038/srep16560.

Okuchi, T. (1997), Hydrogen partitioning into molten iron at high pressure: Implications for Earth's core, *Science*, *278*, 1781–1784, doi:10.1126/science.278.5344.1781.

Pépin, C. M., A. Dewaele, G. Geneste, P. Loubeyre, and M. Mezouar (2014), New iron hydrides under high pressure, *Phys. Rev. Lett.*, *113*, 265504, doi:10.1103/PhysRevLett.113.265504.

Raymond, S. N., T. Quinn, and J. I. Lunine (2007), High-resolution simulations of the final assembly of Earth-like planets. 2. Water delivery and planetary habitability, *Astrobiology*, *7*, 66–84, doi:10.1089/ast.2006.06-0126.

Sakamaki, K., E. Takahashi, Y. Nakajima, Y. Nishihara, K. Funakoshi, T. Suzuki, and Y. Fukai (2009), Melting phase relation of FeH_x up to 20 GPa: Implication for the temperature of the Earth's core, *Phys. Earth Planet. Inter.*, *174*, doi:10.1016/j.pepi.2008.05.017.

Sata, N., G. Shen, M. L. Rivers, and S. Sutton (2002), Pressure-volume equation of state of the high-pressure B2 phase of NaCl, *Phys. Rev. B*, *65*, 104114, doi:10.1103/PhysRevB.65.104114.

Shahar, A., K. Ziegler, E. D. Young, A. Ricolleau, E. A. Schauble, and Y. Fei (2009), Experimentally determined Si isotope fractionation between silicate and Fe metal and implications for Earth's core formation, *Earth Planet. Sci. Lett.*, *288*, 228–234, doi:10.1016/j.epsl.2009.09.025.

Speziale, S., C.-S. Zha, T. S. Duffy, R. J. Hemley, and H.-K. Mao (2001), Quasi-hydrostatic compression of magnesium oxide to 52 GPa: Implications for the pressure-volume-temperature equation of state, *J. Geophys. Res.*, *106*, 515–528, doi:10.1029/2000JB900318.

Tateno, S., Y. Kuwayama, K. Hirose, and Y. Ohishi (2015), The structure of Fe–Si alloy in Earth's inner core, *Earth Planet. Sci. Lett.*, *418*, 11–19, doi:10.1016/j.epsl.2015.02.008.

Terasaki, H., Y. Shibazaki, T. Sakamaki, R. Tateyama, E. Ohtani, K.-I. Funakoshi, and Y. Higo (2011), Hydrogenation of FeSi under high pressure, *Am. Mineral.*, *96*, 93–99, doi:10.2138/am.2011.3628.

Terasaki, H., et al. (2012), Stability of Fe-Ni hydride after the reaction between Fe-Ni alloy and hydrous phase (δ-AlOOH) up to 1.2 Mbar: Possibility of H contribution to the core density deficit, *Phys. Earth Planet. Inter.*, *194-195*, 18–24, doi:10.1016/j.pepi.2012.01.002.

Vočadlo, L., D. Alfè, M. J. Gillan, and G. D. Price (2003), The properties of iron under core conditions from first principles calculations, *Phys. Earth Planet. Inter.*, *140*, 101–125, doi:10.1016/j.pepi.2003.08.001.

Walsh, K. J., A. Morbidelli, S. N. Raymond, D. P. O'Brien, and A. M. Mandell (2011), A low mass for Mars from Jupiter's early gas-driven migration, *Nature*, *475*, 206–209, doi:10.1038/nature10201.

Yamakata, M., T. Yagi, W. Utsumi, and Y. Fukai (1992), In situ X-ray observation of iron hydride under high pressure and high temperature, *Proc. Japan Acad. Ser. B*, *68*, 172–176, doi:10.2183/pjab.68.172.